

## CANGAROO

MASAKI MORI FOR THE CANGAROO-II,III TEAM\*

*Institute for Cosmic Ray Research, University of Tokyo,  
5-1-5 Kashiwanoha, Kashiwa, Chiba 277-0882, Japan  
E-mail: morim@icrr.u-tokyo.ac.jp*

The CANGAROO-III telescope system for very-high-energy gamma-ray astrophysics consists of four 10 m atmospheric Cherenkov telescopes located near Woomera, South Australia. The construction of the fourth telescope was completed in summer 2003, and stereoscopic observations with a local trigger system started in March 2004. Here we report on the status of the system and preliminary results from stereo observations.

### 1. Introduction

CANGAROO is an acronym for the Collaboration of Australia and Nippon (Japan) for a GAMMA Ray Observatory in the Outback, and is a joint project of Japanese and Australian institutions. After the operation of the 3.8 m imaging Cherenkov telescope (CANGAROO-I) for 7 years, which was the first of this kind in the southern hemisphere, we constructed a new telescope of 7 m diameter (CANGAROO-II) in 1999 <sup>1</sup> next to the 3.8m telescope near Woomera, South Australia (136°47'E, 31°06'E, 160m a.s.l.). Then the construction of an array of four 10 m telescope (CANGAROO-III) was approved and as the first step the 7 m telescope was upgraded to 10m diameter in 2000, which is the first telescope of the CANGAROO-III array <sup>2</sup>. In the following years, we have constructed additional three 10m telescopes located at the corners of a diamond of 100m side with improved mirrors, cameras and electronics. After tuning, we have started observation with the full system in stereo mode in March 2004.

---

\*see <http://icrhp9.icrr.u-tokyo.ac.jp/> for the collaboration list.

## 2. The CANGAROO-II telescope

After years of observations with the 3.8 m telescope, which was retrospectively called CANGAROO-I, a new budget to construct a whole new telescope was approved in 1995 <sup>1</sup>. This telescope, CANGAROO-II, was equipped with a reflector <sup>3</sup> consisting of sixty spherical mirrors of 80 cm in diameter, which is approximately 7 m aperture, with a focal length of 8m. The base material of the mirror is CFRP (carbon-fiber reinforced plastic), which was newly developed for use in Cherenkov telescopes, and makes the reflector light and reduces gravitational deformation of the parabola shape. The altitude of each mirror is remotely adjusted by stepping motors. The 7 m telescope began operation in March 1999. In 1999 we obtained a new budget to construct an array of four 10 m telescopes, which is now called CANGAROO-III <sup>2</sup>. As the first step of CANGAROO-III, the 7m telescope was expanded to 10m by addition of 54 mirrors in March 2000, which is called 'T1' after installation of other telescopes. Basic specifications of T1 are given in Table 1.

## 3. Some results from CANGAROO-II

### 3.1. *Supernova remnant RX J1713.7-3946*

The first result from the CANGAROO-II telescope was published in Nature in April, 2002 <sup>4</sup>. A gamma-ray signal was found near the northwest rim of the supernova remnant (SNR) RX J1713.7-3946 (G347.3-0.5) using 2,332 min. on-source and 1,789 min. off-source data in 2000 and 2001. We argued that it could be evidence for the production of gamma-rays by non-electromagnetic process in the SNR using the observed spectrum which was expressed by a single power law and was not compatible with spectra assuming electromagnetic processes: inverse Compton scattering or bremsstrahlung. If it is interpreted as gamma-rays derived from pion decay

Table 1. Basic specification of CANGAROO-III telescopes.

	T1	T2, T3, T4
Mount		Alt-azimuth
Focal length		8m
Number of mirrors		114 (57m <sup>2</sup> in total)
Reflector type		Parabola
Number of PMTs	552 (1/2")	427 (3/4")
Camera pixel size	0.115°	0.168 °
Readout	TDC(CAMAC) & ADC	TDC(VME) & ADC
Point image size	0.20° (FWHM)	0.14 ~ 0.21° (FWHM)
Completion	2000.3	2002.3 (T2), 2002.11 (T3), 2003.7 (T4)

process, this can be the first evidence of proton acceleration in supernova remnants, which might prove the SNR origin of cosmic rays. New H.E.S.S. results on this SNR <sup>5</sup> essentially support this interpretation.

### **3.2. *The Galactic Center***

The Galactic center is one of the most attractive objects in the southern sky. Based on 4,000 min. (ON) and 3,400 min. (OFF) data with CANGAROO-II in 2001 and 2002, we detected a gamma-ray signal at energies greater than 250 GeV <sup>6</sup>. With detections by the Whipple <sup>7</sup> and H.E.S.S. <sup>8</sup> groups, now the Galactic center is an established TeV source. However, the CANGAROO-II spectrum seems to be steeper than that of H.E.S.S.: we will re-observe it with the CANGAROO-III stereo system in 2005.

### **3.3. *Supernova remnant RX J0852.0-4622***

This SNR, sometimes called as “Vela Jr.” or G266.2-1.2, is a SNR located (in projection) at the southeast corner of the Vela SNR. It was discovered in 1998 using data from the ROSAT All-Sky Survey, and it is one of the few known SNRs which display strong non-thermal X-ray emission. With 5900 min. (ON) and 5300 min. (OFF) observations in 2001/2002 and 2003, we found a gamma-ray signal around the peak of the X-ray emission at energies greater than 500 GeV <sup>9</sup>. Again the spectrum seems to be steeper than that of H.E.S.S. <sup>10</sup>, but the extended signal detected by the stereo observation in 2004 shows a harder spectrum when the whole emission region is taken into account (see 5.4).

## **4. The CANGAROO-III system**

### **4.1. *Basic specification***

In 2002-2004 we have installed three new 10 m telescopes (‘T2’, ‘T3’ and ‘T4’) at the corners of a diamond of 100 m sides. This telescope array is called CANGAROO-III <sup>2</sup>. The major parameters of the CANGAROO-III telescopes are summarized in Table 1. The details of the system are described elsewhere <sup>11</sup>. Here we mention some recent updates <sup>12</sup>.

### **4.2. *Star tracking accuracy***

Telescopes are driven by commands specifying elevation and azimuth angles sent to telescope controllers every 100 ms. Those values are computed from

the celestial position of a target object by a control PC synchronized to a master PC equipped with a GPS receiver via `ntp` protocol.

Tracking accuracy of telescopes are monitored using CCD cameras mounted at the center of reflectors and faced to cameras. We can observe stars through the telescope focal ring when cameras are not installed and around the ring when cameras are installed with a wide camera lens. The root-mean-square deviation of displacement between observed and commanded positions is less than one arcminute, which is small enough compared with the size of a camera pixel ( $0.115^\circ$  [T1] or  $0.168^\circ$  [T2, T3, T4]).

### 4.3. *Optical quality*

Each spherical mirror, made of laminates of fiber-reinforced-plastic and aluminium sheet<sup>3</sup>, can have their direction adusted by two stepping motors. Mirrors of the first telescope were tuned using a distant light source<sup>3</sup>. For later (T2, T3, T4) telescopes we tuned mirrors to a common focus while stars were being tracked<sup>13</sup>. Focal images are captured by a CCD camera mounted at the center of the reflector before and after movements of motors and we can identify the displacement of each mirror by subtracting those images. By repeating this procedure on each mirror, we could tune all mirrors in a few nights per telescope. The point spread functions measured at the construction time are  $0.20^\circ$ ,  $0.21^\circ$ ,  $0.14^\circ$ , and  $0.16^\circ$  (FWHM). They are not as good as those of glass-made mirrors, but are comparable with the size of camera pixels.

### 4.4. *Muon rings*

We selected ‘good muon’ events to study the performance of our telescopes in the following criteria: 1) there is a cluster with enough number of adjacent hits in the image; 2) *arclength*, or ring radius times arc angle, is larger than 2 deg-rad; 3) the ring fit is fairly good (small  $\chi^2$ ). The curvature distribution for these muon events shows a clear peak around  $1/1.2^\circ$ , which corresponds to local muons. We studied these muon events in detail and they are used to understand the performance of our telescopes<sup>14</sup>.

### 4.5. *Global trigger system*

Since March 2004 we introduced a “global” trigger system which requires real-time coincidence between telescopes. For each telescope, when a local trigger is generated, data from the electronics are kept for 5  $\mu$ s and at the

same time the local trigger is sent to the stereo trigger system through an optical link. In the stereo trigger system, determination of stereo events is done by requiring any two or three local trigger signals coinciding with each other for at least 10 ns within a 650 ns time window considering the geometrical time delay which depends on the arrival direction of Cherenkov light. When a stereo event is detected, a global trigger signal is generated, and the event number and timing information are recorded. Then, the generated global trigger signal and event number are sent to each telescope. At each telescope, when the global trigger signal is received within 5  $\mu$ s, ADC and TDC data are read out and recorded. If not, the data for that event are cleared, and the electronics and local trigger system are reset for a next event. Using this trigger system, local muon signal, which is evident in the length/size distribution taken in local triggers, disappear and we can reduce the local trigger threshold level in order to decrease the energy threshold.

## 5. Preliminary results from CANGAROO-III

### 5.1. *The Crab nebula*

From Woomera, the Crab nebula can be observed only at large zenith angles ( $> 53^\circ$ ). For stereo observations, The threshold energy of T1 is higher than other telescopes and thus we used the newer three telescopes for analysis. Because of the geometrical arrangement of the array, the effective baseline for large zenith angle observations becomes short which makes stereo reconstruction of images difficult.

To overcome the unfortunate situation described above, we developed new analysis methods. To avoid the increased uncertainty of the intersection points, we introduced a new parameter, “IP distance” ( $D_{IP}$ ), which is defined as the distance between the intersection point and centroid of images. Then we searched best intersection points which minimizes the image widths and the difference between distance and  $D_{IP}$ . This results in better angular resolution as seen in the  $\theta^2$  distribution in Monte Carlo simulations, where  $\theta$  is the space angle between the source direction and the reconstructed arrival direction.

We observed the Crab nebula for 18.5 hours in December 2003 in so-called wobble mode, changing the pointing directions  $\pm 0.5^\circ$  in declination apart from the target every 20 minutes.

In addition to the conventional square cuts method using image parameters to enhance gamma-ray fractions, we applied two different analyses:

the Likelihood method<sup>15,4</sup> and the Fisher Discriminant method. In the latter method, effectiveness of the parameters for the gamma-ray-like event selection is evaluated using the simulation, and we can optimize the weights of the parameters in estimating the probability of gamma-ray-like events. Finally we obtained the spectrum of the Crab nebula in the energy range from 2 to 20 TeV, which is consistent within the statistical and systematic errors with other measurements<sup>16,14</sup>.

### 5.2. *Cen A*

Centaurus A is a well-known radio galaxy and the nearest ( $z = 0.00183$ ) active galactic nucleus. Although its jet axis may be inclined from our line-of-sight, its proximity may overcome the misalignment and it could be detectable in the TeV region. Indeed, it was reported as a TeV gamma-ray source about thirty years ago when it was at a high state<sup>17</sup>. We observed Cen A for 1,047 min. and 882 min. for T2-T3 and T2-T4 pairs, respectively, in 2004 March. The stereo-mode analysis in each pair did not show a gamma-ray signal in the signal region ( $\theta^2 < 0.047^\circ$ ) and we obtained an upper limit of  $3.2 \times 10^{-12} \text{ cm}^{-2}\text{s}^{-1}$  for  $E_\gamma > 530 \text{ GeV}$  ( $2\sigma$  level)<sup>18</sup>.

### 5.3. *The Galactic diffuse emission*

The Galactic plane is the strongest source of gamma-rays in the GeV region. The dominant mechanism of this emission is believed to be the nuclear gamma-rays via neutral pion decays produced in collision of cosmic-rays with interstellar medium. The EGRET results showed harder ( $\propto E^{-2.4\sim 2.5}$ ) spectrum expected from the cosmic-ray origin ( $\propto E^{-2.7}$ )<sup>19</sup>, and if this spectrum extends to the TeV region, this Galactic diffuse emission could be detectable with Cherenkov telescopes. In 2004 we observed two local maximum regions of the diffuse Galactic emission model developed by the EGRET team<sup>19</sup>:  $(\ell, b) = (-19.5^\circ, 0.0^\circ)$  and  $(+13.0^\circ, 0.0^\circ)$ . For the former point,  $b = \pm 3.0^\circ$  were used as off-source regions, and the latter point was observed in long ON-OFF mode. ON-source observations of 10.6 hours ( $\ell = -19.5^\circ$ , T2-T3), 6.3 hours ( $\ell = -19.5^\circ$ , T2-T4), 8.0 hours ( $\ell = +13^\circ$ , T2-T3), and 8.5 hours ( $\ell = +13.5^\circ$ , T2-T4) were analyzed, but we could not find a gamma-ray signal associated with the Galactic disk in both regions. Assuming that the gamma-ray spectrum shows a single power-law between a few GeV and 600 GeV, conservative upper limits to the spectral index were obtained:  $-2.17$  and  $-2.12$  (preliminary) for each region, respectively<sup>20</sup>.

#### 5.4. *Supernova remnant RX J0852.0-4622*

We applied the Fisher discriminant method to the stereo data for RX J0852.0-4622 observed in January and February 2004 using T2 and T3 taken in the wobble mode for 2,197 minutes in total. We used the northwest rim as a target point in the wobble mode. After the coarse selections, 1,204 minutes data was available. For the Fisher discriminant, we used four image parameters, lengths and widths, determined with each telescope independently. Finally the gamma-ray events was extracted by comparing the Fisher discriminant values between the SNR region and the background region. The excess count map is shown in Figure 1. The region inside the solid arcs shows the maximum acceptance region, which is an overlap of the two field-of-views in the wobble mode. Also the one-degree arc from the SNR center is indicated by the dotted line. The strong gamma-ray emission from the NW rim is obviously seen, which was first reported by CANGAROO-II. This maximum acceptance region covers about a half of the whole SNR, and the integrated flux above 0.81 TeV is about 60% of the H.E.S.S. result<sup>10</sup>, which value is reasonable considering our coverage of the SNR<sup>21,22</sup>.

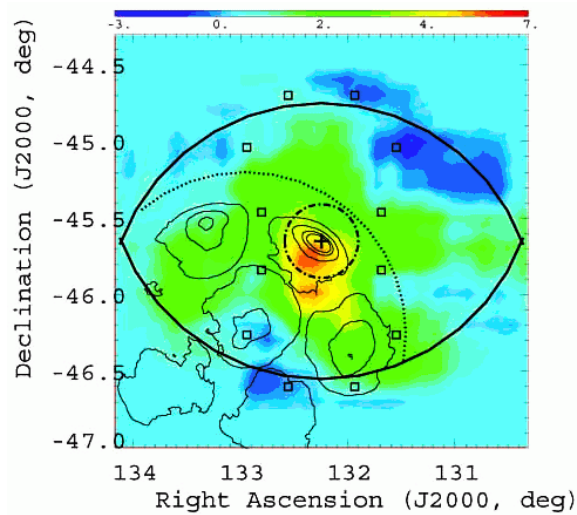


Figure 1. Excess event map around the SNR RX J0852.0-4622 obtained from the CANGAROO-III stereo observations (preliminary).

### 5.5. Other sources

We took fair amount of stereo data on the pulsar PSR 1706-44 and the supernova remnant SN1006 which we claimed to be TeV gamma-ray sources with CANGAROO-I. Preliminary analysis of both objects did not show any peaks in the  $\theta^2$  distribution<sup>21</sup>. (For SN1006 we take the northwest rim point where TeV gamma ray emission was reported by CANGAROO-I as the emission point.) Further analysis is underway so that we can check the possible extended emission.

## 6. Summary

We have been carrying out stereo observations of sub-TeV gamma-rays with four telescopes since March 2004. Preliminary results from stereo observations were presented here: further results are coming soon.

## References

1. T. Tanimori et al., in *Proc. 26th ICRC (Utah)* (University of Uta, Utah), **5**, 203–206 (1999).
2. H. Kubo et al., *New Astronomy Reviews* **48**, 323–329 (2004).
3. A. Kawachi et al., *Astropart. Phys.* **14**, 261–269 (2001).
4. R. Enomoto et al., *Nature* **416**, 823–826 (2002).
5. F.A. Aharonian et al., *Nature* **432**, 75–77 (2004).
6. K. Tsuchiya et al., *Astrophys. J.* **606**, L115–L118 (2004).
7. K. Kosack et al., *Astrophys. J.* **608**, 97 (2004).
8. F. Aharonian et al., *Astron. Astrophys.* **425**, L13–L17 (2004).
9. H. Katagiri et al., *Astrophys. J.* **619**, L163–L165 (2005).
10. F. Aharonian et al., *Astron. Astrophys.* **437**, L7–L10 (2005).
11. R. Enomoto et al., in *Proc. 28th ICRC (Tsukuba)* (Universal Academy Press, Tokyo), pp. 2807–2810 (2003) and references therein.
12. K. Nishijima et al., in *Proc. 29th ICRC (Pune)*, in press (2005).
13. M. Ohishi et al., in *Proc. 28th ICRC (Tsukuba)* (Universal Academy Press, Tokyo), pp. 2855–2858 (2003).
14. R. Enomoto et al., submitted for publication (2005).
15. R. Enomoto et al., in *Proc. 27th ICRC (Hamburg)* (Copernicus Gesellschaft, Germany), Vol.5, pp. 2477–2480 (2001).
16. T. Nakamori et al., in *Proc. 29th ICRC (Pune)*, in press (2005).
17. J.E. Grindlay et al., *Astrophys. J.* **201**, 82–89 (1975).
18. S. Kabuki et al., in *Proc. 29th ICRC (Pune)*, in press (2005).
19. S.D. Hunter et al., *Astrophys. J.* **481**, 205–240 (1997).
20. M. Ohishi et al., in *Proc. 29th ICRC (Pune)*, in press (2005).
21. T. Tanimori et al., in *Proc. 29th ICRC (Pune)*, in press (2005).
22. R. Enomoto et al., to be submitted for publication (2005).